Electronic Supporting Information

$KSb(BeF_3)F_3$: Totally Fluorine Strategy Achieving Wide Bandgap and Large Birefringence

Xuehua Dong,[a] Ying Long,[b] Ling Huang,*[a] Liling Cao,[a] Daojiang Gao,[a] Jian Bi,[a] and Guohong Zou*[b]

[a] College of Chemistry and Materials Science, Sichuan Normal University, Chengdu, 610066, P. R. China.

[b] College of Chemistry, Sichuan University, Chengdu, 610065, P. R. China.

E-mail: huangl026@sina.com, zough@scu.edu.cn.

Table of contents

Table S1. Atomic coordinates and equivalent isotropic displacement parameters, and calculated Bond Valence Sum for $KSb(BeF_3)F_3$. $U_{(eq)}$ is defined as one third of the trace of the orthogonalized U_{ij} tensor.

atom	x	y	z	U_{eq}(Å^2)	BVS
Sb1	0.63577 (2)	0.38502 (3)	0.43311 (2)	0.01584 (8)	3.07
K1	0.56279 (4)	-0.18109 (15)	0.15299 (5)	0.02744 (14)	0.85
Be1	0.76924 (19)	0.7423 (8)	0.3233 (3)	0.0220 (7)	1.99
F1	0.53872 (9)	0.3033 (4)	0.44162 (13)	0.0246 (3)	1.09
F2	0.58593 (11)	0.3142 (4)	0.28293 (13)	0.0317 (4)	1.11
F3	0.59471 (10)	0.7881 (4)	0.39518 (15)	0.0344 (4)	1.08
F4	0.72684 (16)	0.6374 (5)	0.3860 (2)	0.0630 (7)	0.80
F5	0.78329 (9)	0.4708 (4)	0.26231 (15)	0.0335 (4)	0.63
F6	0.84627 (10)	0.8833 (3)	0.39239 (14)	0.0326 (4)	0.79

Table S2. Selected Bond lengths (Å) and angles (deg) for $KSb(BeF_3)F_3$.

Sb1—F2	1.9340 (16)	K1—F3^{viii}	3.188 (2)
Sb1—F3	1.9310 (16)	K1—F3^{vii}	2.8239 (19)
Sb1—F6^{iv}	2.5379 (18)	K1—F6^{ix}	3.2655 (18)
Sb1—F4	2.400 (2)	K1—F6^{x}	2.8540 (18)
K1—F1^{v}	2.8244 (17)	K1—F5^{ix}	2.7735 (18)
K1—F1^{vi}	2.8514 (17)	F6—Be1	1.521 (4)
K1—F1^{vii}	2.9305 (17)	F4—Be1	1.507 (4)
K1—F2^{viii}	2.7943 (18)	Be1—F5	1.564 (4)
F3—Sb1—F4	76.00 (8)	F3^{vii}—K1—F1^{vi}	93.38 (5)
F4—Sb1—F6^{iv}	105.20 (8)	F3^{vii}—K1—F1^{v}	57.49 (5)
F1^{v}—K1—F1^{vii}	100.36 (5)	F3^{vii}—K1—F3^{viii}	87.35 (5)
F1^{vi}—K1—F1^{vii}	66.39 (5)	F3^{viii}—K1—F6^{ix}	111.35 (5)
F1^{v}—K1—F3^{viii}	108.33 (5)	F3^{vii}—K1—F6^{ix}	127.13 (5)
F1^{vii}—K1—F3^{viii}	103.81 (5)	F6^{x}—K1—F3^{viii}	110.51 (5)
F1^{v}—K1—F6^{x}	140.94 (5)	F6^{x}—K1—F6^{ix}	92.26 (5)
F1^{vi}—K1—F6^{ix}	78.79 (5)	F5^{ix}—K1—F1^{vii}	140.44 (5)
F1^{vii}—K1—F6^{ix}	144.84 (5)	F5^{ix}—K1—F1^{v}	114.90 (5)
F1^{v}—K1—F6^{ix}	69.65 (4)	F5^{ix}—K1—F1^{vi}	99.37 (5)
F1^{vi}—K1—F6^{x}	58.94 (5)	F5^{ix}—K1—F2^{viii}	93.94 (5)
F2^{viii}—K1—F1^{vi}	115.94 (5)	F5^{ix}—K1—F3^{viii}	82.36 (5)
F2—K1—F1^{vii}	143.63 (5)	F5^{ix}—K1—F6^{x}	67.06 (5)
F2—K1—F1^{v}	66.07 (5)	F5^{ix}—K1—F6^{ix}	48.06 (5)
F2—K1—F1^{vi}	138.24 (5)	Sb1—F1—K1^{iii}	111.13 (7)
F2^{viii}—K1—F1^{v}	142.99 (5)	Sb1—F1—K1^{v}	126.96 (7)
F2—K1—F2^{viii}	105.44 (6)	Sb1—F1—K1^{i}	107.55 (6)
F2—K1—F3^{vii}	92.97 (5)	K1^{v}—F1—K1^{i}	100.36 (5)
F2^{viii}—K1—F3^{viii}	50.63 (4)	K1^{v}—F1—K1^{iii}	96.84 (5)
F2^{viii}—K1—F3^{vii}	88.57 (6)	Sb1—F2—K1ii	116.69 (7)
F2—K1—F6^{x}	137.73 (6)	Sb1—F2—K1	135.52 (8)
F2^{viii}—K1—F6^{x}	70.36 (5)	K1—F2—K1^{ii}	105.44 (6)
F2^{viii}—K1—F6^{ix}	141.92 (5)	Sb1—F3—K1^{i}	112.62 (7)
F2—K1—F5^{ix}	71.45 (6)	K1^{i}—F3—K1^{ii}	92.41 (5)
F3^{vii}—K1—F1^{vii}	53.79 (4)	Sb1iv—F6—K1xi	129.20 (7)
F6—Be1—F5	108.3 (2)	Sb1^{iv}—F6—K1^{xii}	95.63 (5)
F4—Be1—F6	112.4 (3)	K1^{xii}—F6—K1^{xi}	92.26 (5)
F4—Be1—F5^{xi}	108.1 (2)	Be1—F6—K1^{xii}	131.45 (16)
F5—Be1—F5^{xi}	106.3 (2)	Be1—F6—K1^{xi}	91.36 (15)
Be1—F5—K1^{xi}	110.78 (15)	Be1—F4—Sb1	161.3 (2)
Be1^{ix}—F5—K1^{xi}	113.50 (14)	F6—Be1—F5^{xi}	111.3 (2)

Symmetry codes: (i) -*x*+1, *y*+1, -*z*+1/2; (ii) *x*, *y*+1, *z*; (iii) *x*, -*y*, *z*+1/2; (iv) -*x*+3/2, -*y*+3/2, -*z*+1; (v) -*x*+1, *y*, -*z*+1/2; (vi) *x*, -*y*, *z*-1/2; (vii) -*x*+1, *y*-1, -*z*+1/2; (viii) *x*, *y*-1, *z*; (ix) -*x*+3/2, *y*-1/2, -*z*+1/2; (x) -*x*+3/2, *y*-3/2, -*z*+1/2; (xi) -*x*+3/2, *y*+1/2, -*z*+1/2; (xii) -*x*+3/2, *y*+3/2, -*z*+1/2.

Table S3. Anionic structures and band gap of most reported antimony-based inorganic optical crystals.

Compounds	Anionic groups	Band gaps (eV)	Ref.
$KSb(BeF_3)F_3$	1D $[BeF_3]^-_\infty$	5.3	This work
$Na_2SO_4 \cdot SbF_3$	isolated SO_4	5.13	[1]
$Rb_6Sb_4F_{12}(SO_4)_3$	isolated SO_4	5.07	[2]
$NH_4SbFPO_4 \cdot H_2O$	isolated PO_4	5.01	[3]
$Cs_6Sb_4F_{12}(SO_4)_3$	isolated SO_4	4.97	[2]
$CsSbF_2SO_4$	isolated SO_4	4.76	[4]
$K_2Sb(P_2O_7)F$	P_2O_7 dimer	4.75	[5]
$RbSbF_2SO_4$	isolated SO_4	4.75	[6]
$K_2SO_4 \cdot (SbF_3)_2$	isolated SO_4	4.73	[7]
$Rb_2SO_4 \cdot (SbF_3)_2$	isolated SO_4	4.69	[7]
$NH_4SbF_2SO_4$	isolated SO_4	4.67	[3]
$(NH_4)_2SbCl(SO_4)_2$	isolated SO_4	4.56	[8]
$(NH_4)_2SO_4 \cdot SbF_3$	isolated SO_4	4.54	[1]
$NH_4SbCl_2SO_4$	isolated SO_4	4.54	[8]
$K_2SO_4 \cdot SbF_3$	isolated SO_4	4.44	[1]
$Ba_3Sb_2(PO_4)_4$	isolated PO_4	4.30	[9]
$K_2Sb_2(C_2O_4)F_6$	isolated C_2O_4	4.27	[10]
$Rb_2SO_4 \cdot SbF_3$	isolated SO_4	4.15	[1]
$K_4Sb(SO_4)_3Cl$	isolated SO_4	4.12	[11]
$[C(NH_2)_3]Sb(C_2O_4)F_2 \cdot H_2O$	isolated C_2O_4	4.09	[17]
$KSb_2C_2O_4F_5$	isolated C_2O_4	4.06	[12]
$Na_2Sb_2(C_2O_4)F_6$	isolated C_2O_4	4.03	[10]
$NH_4Sb_2(C_2O_4)F_5$	isolated C_2O_4	3.85	[13]
$RbSb(C_2O_4)F_2 \cdot H_2O$	isolated C_2O_4	3.83	[17]
$Cs_2Sb_2(C_2O_4)F_4 \cdot H_2O$	isolated C_2O_4	3.81	[10]
$Rb_2SbF_3(NO_3)_2$	isolated NO_3	3.76	[14]
$Rb_3SbF_3(NO_3)_3$	isolated NO_3	3.75	[15]
$RbSbSO_4Cl_2$	isolated SO_4	3.48	[16]

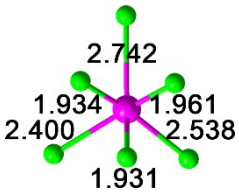

Fig. S1 The bond lengths of SbF_6 octahedron in $KSb(BeF_3)F_3$.

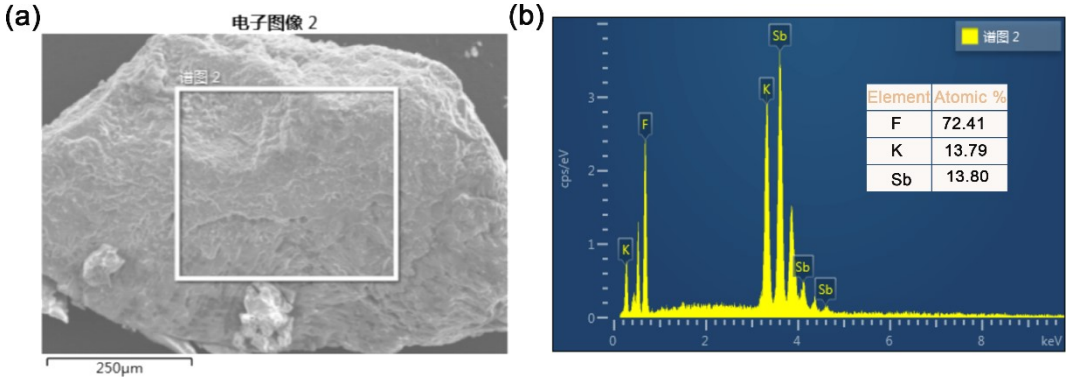

Fig. S2 Energy-dispersive analysis by X-ray (EDX) data for $KSb(BeF_3)F_3$.

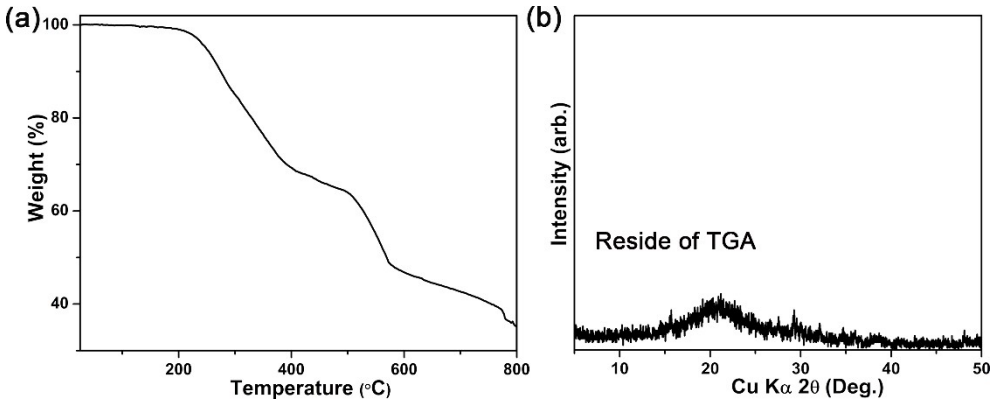

Fig. S3 (a) The TGA spectrum for $KSb(BeF_3)F_3$; (b) The Powder XRD patterns of the residue of TGA for $KSb(BeF_3)F_3$. The result indicated that the residue of TGA for $KSb(BeF_3)F_3$ has changed to amorphous substance.

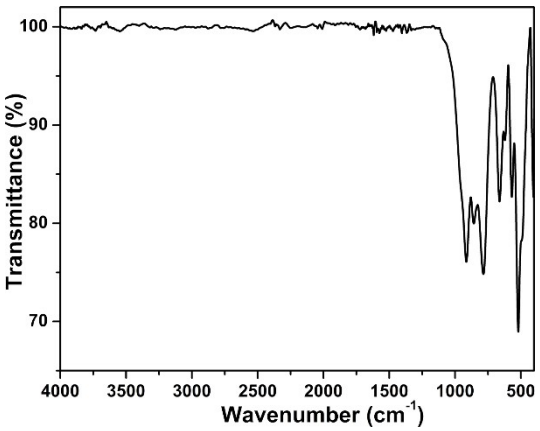

Fig. S4 The IR spectrum for $KSb(BeF_3)F_3$.

References

[1] He, F. F.; Wang, L.; Hu, C. F.; Zhou, J.; Li, Q.; Huang, L.; Gao, D. J.; Bi, J.; Wang, X.; Zou, G. H. Cation-tuned synthesis of the $A_2SO_4{\cdot}SbF_3$ ($A = Na^+, NH_4^+, K^+, Rb^+$) family with nonlinear optical properties. *Dalton Trans.* **2018**, *47*, 17486-17492.

[2] Dong, X. H.; Long, Y.; Zhao, X. Y.; Huang, L.; Zeng, H. M.; Lin, Z. E.; Wang, X.; Zou, G. H. $A_6Sb_4F_{12}(SO_4)_3$ (A = Rb, Cs): Two novel antimony fluoride sulfates with unique crown-like clusters. *Inorg. Chem.* **2020**, *59*, 8345-8352.

[3] He, F. F.; Ge, Y. W.; Zhao, X. Y.; He, J.; Huang, L.; Gao, D. J.; Bi, J.; Wang, X.; Zou, G. H. Two-stage evolution from phosphate to sulfate of new KTP-type family members as UV nonlinear optical materials through chemical cosubstitution-oriented design. *Dalton Trans.* **2020**, *49*, 5276-5282.

[4] Dong, X. H.; Huang, L.; Hu, C. F.; Zeng, H. M.; Lin, Z. E.; Wang, X.; Ok, K. M.; Zou, G. H. $CsSbF_2SO_4$: An excellent ultraviolet nonlinear optical sulfate with a $KTiOPO_4$ (KTP)-type structure. *Angew. Chem. Int. Ed.* **2019**, *58*, 6528-6534.

[5] Deng, Y. L.; Huang, L.; Dong, X. H.; Wang, L.; Ok, K. M.; Zeng, H. M.; Lin, Z. E.; Zou, G. H. $K_2Sb(P_2O_7)F$: Unprecedented cairo pentagonal layer with new bifunctional genes revealing excellent optical performance. *Angew. Chem. Int. Ed.* **2020**, *59*, 21151-21156.

[6] Yang, F.; Huang, L. J.; Zhao, X. Y.; Huang, L.; Gao, D. J.; Bi, J.; Wang, X.; Zou, G. H. An energy band engineering design to enlarge the band gap of $KTiOPO_4$ (KTP)-type sulfates via aliovalent substitution. *J. Mater. Chem. C* **2019**, *7*, 8131-8138.

[7] Wang, Q.; Wang, L.; Zhao, X. Y.; Huang, L.; Gao, D. J.; Bi, J.; Wang, X.; Zou, G. H. Centrosymmetric $K_2SO_4{\cdot}(SbF_3)_2$ and noncentrosymmetric $Rb_2SO_4{\cdot}(SbF_3)_2$ resulting from cooperative effects of lone pair and cation size. *Inorg. Chem. Front.* **2019**, *6*, 3125-3132.

[8] He, F. F.; Wang, Q.; Hu, C. F.; He, W.; Luo, X. Y.; Huang, L.; Gao, D. J.; Bi, J.; Wang, X.; Zou, G. H. Centrosymmetric $(NH_4)_2SbCl(SO_4)_2$ and non-centrosymmetric $(NH_4)SbCl_2(SO_4)$: synergistic effect of hydrogen-bonding interactions and lone-pair cations on the framework structures and macroscopic centricities. *Cryst. Growth Des.* **2018**, *18*, 6239-6247.

[9] Bi, X. B.; Hu, C. L.; Kong, F.; Mao, J. G. $Ba_3Sb_2(PO_4)_4$ and $Cd_3Sb_2(PO_4)_4(H_2O)_2$: Two new antimonous phosphates with distinct $[Sb(PO_4)_2]$ structure types and enhanced birefringence. *Inorg. Chem.* **2021**, *60*, 1957-1964.

[10] Zhang, D.; Wang, Q.; Zheng, T.; Cao, L. L.; Ok, K. M.; Gao, D. J.; Bi, J.; Huang, L.; Zou, G. H. Cation-anion synergetic interactions achieving tunable birefringence in quasi-one-dimensional antimony(III) fluoride oxalates. *Sci. China Mater.* **2022**, 10.1007/s40843-022-2088-0.

[11] Yang, F.; Wang, L.; Ge, Y. W.; Huang, L.; Gao, D. J.; Bi, J.; Zou, G. H. $K_4Sb(SO_4)_3Cl$: The first apatite-type sulfate ultraviolet nonlinear optical material with sharply enlarged birefringence. *J. Alloys Compd.* **2020**, *834*, 155154.

[12] Chen, Y. X.; Chen, Z. X.; Zhou, Y.; Li, Y. Q.; Liu, Y. C.; Ding, Q. R.; Chen, X.; Zhao, S. G.; Luo, J. H. An antimony(III) fluoride oxalate with large birefringence. *Chem. Eur. J.* **2021**, *27*, 4557-4560.

[13] Zhang, D.; Wang, Q.; Zheng, T.; Huang, L.; Cao, L. L.; Gao, D. J.; Bi, J.; Zou, G. H. $NH_4Sb_2(C_2O_4)F_5$: A novel UV nonlinear optical material synthesized in deep eutectic solvents. *J. Alloys Compd.* **2021**, *896*, 162921.

[14] Wang, L.; Wang, H. M.; Zhang, D.; Gao, D. J.; Bi, J.; Huang, L.; Zou, G. H. Centrosymmetric $RbSnF_2NO_3$ vs. noncentrosymmetric $Rb_2SbF_3(NO_3)_2$. *Inorg. Chem. Front.* **2021**, *8*, 3317-3324.

[15] Wang, L.; Yang, F.; Zhao, X. Y.; Huang, L.; Gao, D. J.; Bi, J.; Wang, X.; Zou, G. H. $Rb_3SbF_3(NO_3)_3$: An excellent antimony nitrate nonlinear optical material with a strong second harmonic generation response fabricated by a rational multi-component design. *Dalton Trans*. **2019**, *48*, 15144-15150.

[16] He, F. F.; Deng, Y. L.; Zhao, X. Y.; Huang, L.; Gao, D. J.; Bi, J.; Wang, X.; Zou, G. H. $RbSbSO_4Cl_2$: an excellent sulfate nonlinear optical material generated due to the synergistic effect of three asymmetric chromophores. *J. Mater. Chem. C* **2019**, *7*, 5748-5754.

[17] Zhang, D.; Wang, Q.; Ren, L. Y.; Cao, L. L.; Huang, L.; Gao, D. J.; Bi, J.; Zou, G. H. Sharp Enhancement of Birefringence in Antimony Oxalates Achieved by the Cation−Anion Synergetic Interaction Strategy, *Inorg. Chem.* **2022**, *61*, 12481-12488.